On Closest Isotropic Tensors and Their Norms

by

© *Andrea D. Noseworthy*

A thesis submitted to the

School of Graduate Studies

in partial fulfilment of the

requirements for the degree of

Master of *Science (Geophysics)*

Department of *Earth Sciences*

Memorial University of Newfoundland

March 2018

St. John's Newfoundland

Contents

Abstract

Theoretical seismology, which is the subject of the thesis, could be viewed as a subject of continuum mechanics, whose mathematical structure relies on tensors. For instance, Hooke's Law, which underlies the theory of elasticity—a branch of continuum mechanics—is a tensorial equation. A generally anisotropic tensor, obtained from physical measurements, can be approximated by another tensor belonging to a particular material-symmetry class. This tensor is referred to as the effective tensor; among all tensors in a particular symmetry class, it is the closest to the given anisotropic tensor. This 'closeness' that we refer to, draws upon the notion of a norm. In this thesis, we compare the effective tensors belonging to the isotropic symmetry class obtained using three different norms—the Frobenius-36, the Frobenius-21, and the operator norms. Furthermore, we utilize another method—a 'L_2 slowness-curve fit' method—and compare the results herein. Finally, we explore the associated errors and analyze the relationship between the mathematical and physical models.

Acknowledgements

We wish to acknowledge collaborations and discussions with Dr. Michael Slawinski and his ongoing support, as well as the discussions and editorial support of Theodore Stanoev and Filip Adamus. Furthermore, acknowledgements are given to the discussions with and editorial support of David Dalton, to the discussions with and computational support of Tomasz Danek, and to the discussions with Dr. Mikhail Kotchetov. Also, we wish to acknowledge the graphical support of Elena Patarini. This research was performed in the context of The Geomechanics Project supported by Husky Energy.

List of Tables

List of Figures

List of Abbreviations and Symbols

Abbreviation/Symbol	Meaning
$c_{ijk\ell}$	Elasticity tensor
F_{36}	Frobenius-36 norm
F_{21}	Frobenius-21 norm
λ	Operator norm
α	Thomsen parameter for p-wave speed along symmetry axis
β	Thomsen parameter for s-wave speed along symmetry axis
γ	Thomsen parameter of anisotropy strength
δ	Thomsen parameter of anisotropy strength
ε	Thomsen parameter of anisotropy strength
ρ	Mass density

Review of Pertinent Literature

In the last century, scientists were interested in how to express a generally anisotropic tensor by its closest isotropic counterpart. This means, given anisotropic seismic data in tensor form, we can approximate this tensor to its "closest" isotropic counterpart using a distance or length function that measures the difference between the elastic moduli of two materials. The work of Voigt (1910) provided a method that became a standard to a point that many are not even aware of other approaches. However, the concept of "closeness" is norm-dependent; meaning, the 'closest' isotropic counterpart may differ using different mathematical norms. Voigt *a priori* assumed a pythagorean norm known as a *Frobenius norm*[1]. For an explanation of the Frobenius norm, refer to Section (2.1.1). In this thesis, we compare the Voigt (1910) approach—the Frobenius-36 norm—with other norms. More specifically, the Frobenius-21 and operator norms.

Voigt (1910) introduced the concept of the nearest isotropic tensor, using the Frobenius-36 norm, to a given anisotropic tensor. From here, research in this area of mathematical physics began to move forward.

Preliminary work in the area of tensor analysis had begun and Gazis et al. (1963) put forth a paper on the elastic tensor of given symmetry nearest to an anisotropic elastic tensor. They produce some general theorems concerning tensors of any rank in an n-dimensional *Euclidean space*[2]. They construct the nearest isotropic tensor

[1]The Frobenius norm, which is also called Euclidean norm, provides a natural definition for distance, and using it one can find the elastic tensor of a given symmetry nearest to an anisotropic elastic tensor.

[2]Euclidean n-space, sometimes called Cartesian space or simply n-space, is the space of all n-

to a given anisotropic elastic tensor as well as to the nearest cubic tensor. They also discuss how the theorems presented can be applied to other symmetry groups of crystals.

Norris (2006) states in his paper that the isotropic elastic moduli closest to a given anisotropic elasticity tensor can be defined using the Frobenius norm, the Riemannian distance for tensors, and the *log-Euclidean metric*[3]. He concludes that the closest moduli are unique for both the Riemannian and log-Euclidean norms.

Moakher and Norris (2006) put forth a paper discussing solutions for the Frobenius, Riemannian, and log-Euclidean distance functions. They pay particular attention to the Riemannian and log-Euclidean functions as their solutions are invariant under inversion, where the Frobenius distance is not. They investigate the three metrics at a level greater than Norris (2006).

Kotchetov and Slawinski (2009) investigate obtaining effective transversely isotropic elasticity tensors. They use the Frobenius norm and formulate a method for finding the optimal orientation of the coordinate system, which is the one that produces the shortest distance.

Danek and Slawinski (2014) investigate another norm—the "operator" norm—to view how effective it is in finding the effective transversely isotropic tensor from a

---

tuples of real numbers—(x_1, x_2, ..., x_n). The term "Euclidean" distinguishes these spaces from other types of spaces considered in modern geometry. Euclidean spaces also generalize to higher dimensions. (High-dimensional spaces frequently occur in mathematics and the sciences. They may be parameter spaces or configuration spaces such as in Lagrangian or Hamiltonian mechanics; these are abstract spaces, independent of the physical space we live in.)

[3]For further reading on the Riemannian distance and the log-Euclidean metric, see Arsingy et al. (2006)).

given anisotropic tensor. In this paper, they compare the effective tensors belonging to the transversely isotropic class obtained using two different norms: the Frobenius-36 and the operator norm.

Bos and Slawinski (2014) investigate the same two norms described previously—the Frobenius-36 and operator norms—and use them to measure distances between a given anisotropic tensor and its closest effective isotropic counterparts.

The concept of a norm is a standard subject in mathematics. In light of this, certain technical details used in this thesis originate from mathematical textbooks. In this thesis, we make use of Horn and Johnson (2013) in their discussion on matrix norms. Also, we use Lancaster and Tismenetsky (1985), particularly their discussion on induced matrix norms, as well as Wilkinson's (1965) ideas on eigenvalues of matrices of condensed forms.

Preface

Introduction

The symmetry class of an elasticity tensor is a property of a Hookean solid, defined by that tensor. Such a solid might serve as a mathematical analogy of a physical material. An elasticity tensor obtained from seismic measurements subject to experimental errors, and without an *a priori* assumed material symmetry, is anisotropic. The inference of properties of a physical material requires further interpretation of this generally anisotropic elasticity tensor. Among these properties are its symmetries. In particular, it is useful to compute an isotropic counterpart of the obtained tensor, which might be sufficiently accurate for seismic interpretations, while offering a significant mathematical convenience. The decision then lies in choosing an appropriate norm to compute such a counterpart, which is the crux of this study. An examination of several norms to obtain an isotropic counterpart is presented by Norris (2006). Herein, we numerically compare isotropic counterparts according to the Frobenius-36 norm, Frobenius-21 norm, which we refer to as F_{36} and F_{21}, respectively, as well as according to the operator norm and the L_2 slowness-curve fit, which we refer to as λ and L_2, respectively. Also, we use perturbation techniques to examine the effect of errors on isotropic counterparts. We finish the investigation by discussing the satisfaction of stability conditions or, more generally, the relation between the mathematical and physical models.

Rudiments

This study is set up in such a fashion where we begin with discussions of the pertinent physical basics — balance principles, deformations and material symmetry. To further that, we have discussions of the pertinent mathematical basics — different types of norms, and the concept of slowness curve L_2 fit. We then introduce numerical models, applying the prior discussed notions, and compare the results. Furthermore, we investigate the related error propagation and, finally, the relation between the mathematical and physical models. As the reader moves through this study, it should be noted that boldface terms are emphasized and are discussed further in the glossary. Italicized terms are other concepts that are pertinent to this study and may be elaborated on in the provided footnotes.

Chapter 1

Continuum Mechanics

1.1 Introduction

Continuum mechanics is a branch of mechanics that pertains to the study of deformations. As stated by the qualifier continuum, the study disregards the discrete atoms of matter. This approximation allows us to remain within the concept of continuity, allowing for the application of calculus. As a result, continuum mechanics is able to model physical phenomena with great success. Among other applications, we may study the field of quantitative seismology using continuum mechanics.

Such an approximation may be thought of as unwise, especially where adjacent elements are not perceptibly different from each other, due to boundaries. However, such approximations have proven useful in scientific study and have allowed for the application of mathematical physics to the study of physical phenomena. On length-scales, much greater than that of inter-atomic distances, such models are highly accurate. This approximation opens many avenues of computation and application to models

of solids, liquids, and gases.

The concept of a continuous function allows differentiability. More specifically, we can define stress and strain at given points and can apply methods of calculus to the study of forces and their interactions.

1.2 Material Symmetry

1.2.1 Introductory Remarks

The concept of symmetry is an integral part of both mathematics and physics. In this section, we focus on rotational symmetries of Hookean solids, which is part of the subject of anisotropy. A Hookean solid, $c_{ijk\ell}$, is a mathematical entity. It relates stress, σ_{ij}, and strain, $\varepsilon_{k\ell}$, in a linear fashion. This linear relationship is known as Hooke's Law and is described as

$$\sigma_{ij} = \sum_{k=1}^{3} \sum_{\ell=1}^{3} c_{ijk\ell} \varepsilon_{k\ell} \,, \qquad i, j \in \{1, 2, 3\} \,. \tag{1.1}$$

Since these solids can be described as mathematical entities, we describe such a symmetry as a mathematical concept. Heuristically, mathematical symmetries mean that we can perform operations on an object without modifying its appearance. For example, a sphere may be rotated about any axis by any amount and its appearance will stay the same. Similarly, within an isotropic Hookean solid, wave-propagation properties are independent of its orientation, thus giving them symmetry that is synomous to that of a sphere. This invariance to the orientation of the coordinate system is called material symmetry. To forward this notion to physical phenomena, such a

behavior is a good analogy for granites, as they show a randomized arrangement of quartz, mica, and feldspar. Shales, however, are different in the sense that properties of disturbances propagating along laminations might be quite different from properties of disturbances propagating obliquely to laminations. Hence, physical materials exhibit differing symmetries.

Herein, $c_{ijk\ell}$ are the components of an elasticity tensor; a 6×6 symmetric[1], positive-definite matrix, belonging to a particular symmetry class. For the purpose of this study, the components of an elasticity tensor belong to one of the three symmetry classes described in section (1.2.3).

1.2.2 Symmetry Conditions

Material symmetries can be studied using a transformation of an orthonormal coordinate system in the $x_1x_2x_3$-space. We are specifically interested in distance-preserving transformations, as these transformations allow us to change the orientation of the continuum without deforming it.

The invariance to an orthogonal transformation imposes certain conditions on the elasticity matrix. For the transformed and the original matrices to be identical to one another, they must possess a particular form. Here, we study a method where, given an orthogonal transformation, we can find the elasticity matrix that is invariant under this transformation, and hence, describe the material symmetry exhibited by

[1]Refer to section 3.2.2 of Slawinski, 2015, for an explanation of how the elasticity tensor, $c_{ijk\ell}$, is invariant under permutations in the first pair of subscripts, as well as under permutations in the second pair of subscripts, thus giving the number of independent components of the elasticity tensor, $c_{ijk\ell}$, to be thirty-six.

a particular continuum. This method is stated in the theorem that follows.

Theorem 1. *The elastic properties of a continuum are invariant under an orthogonal transformation, given by matrix A, if and only if*

$$C = M_A^T \, C \, M_A \,, \tag{1.2}$$

where C is the elasticity matrix and M_A is the transformation matrix.

For a complete proof of this theorem, refer to Slawinski (2015, page 144). The topic of material symmetries and their classes will be expanded in section (3.1).

1.2.3 Tensor Forms

Due to the existence of the strain-energy function and under the assumption of the equality of mixed partial derivatives

$$c_{ijk\ell} = c_{k\ell ij} \,, \qquad i,j,k,\ell \in \{1,2,3\} \,, \tag{1.3}$$

where $c_{ijk\ell}$ are entries of elasticity tensor C from equation (1.2). Expression (1.3) reduces the thirty-six components of a 6×6 elasticity matrix to twenty-one independent components[2]. They can be written—in Kelvin's, as opposed to Voigt's, notation—as entries $c_{ijk\ell}$ of a 6×6 symmetric second-rank tensor in $\mathbb{R}^6$.

A generally **anisotropic** tensor is the most general tensor described by stress-strain equations[3] and is denoted as

[2]For further insight into the strain-energy function, refer to Slawinski (2015, page 116).

[3]For further insight into the formulation of stress-strain equations, refer to Slawinski (2015, page 90).

$$C^{\text{aniso}} = \begin{bmatrix} c_{1111} & c_{1122} & c_{1133} & \sqrt{2}c_{1123} & \sqrt{2}c_{1113} & \sqrt{2}c_{1112} \\ c_{1122} & c_{2222} & c_{2233} & \sqrt{2}c_{2223} & \sqrt{2}c_{2213} & \sqrt{2}c_{2212} \\ c_{1133} & c_{2233} & c_{3333} & \sqrt{2}c_{3323} & \sqrt{2}c_{3313} & \sqrt{2}c_{3312} \\ \sqrt{2}c_{1123} & \sqrt{2}c_{2223} & \sqrt{2}c_{3323} & 2c_{2323} & 2c_{2313} & 2c_{2312} \\ \sqrt{2}c_{1113} & \sqrt{2}c_{2213} & \sqrt{2}c_{3313} & 2c_{2313} & 2c_{1313} & 2c_{1312} \\ \sqrt{2}c_{1112} & \sqrt{2}c_{2212} & \sqrt{2}c_{3312} & 2c_{2312} & 2c_{1312} & 2c_{1212} \end{bmatrix}. \tag{1.4}$$

Using matrix (1.4), equation (1.1) can be rewritten as

$$\begin{bmatrix} \sigma_{11} \\ \sigma_{22} \\ \sigma_{33} \\ \sqrt{2}\sigma_{23} \\ \sqrt{2}\sigma_{13} \\ \sqrt{2}\sigma_{12} \end{bmatrix} = \begin{bmatrix} c_{1111} & c_{1122} & c_{1133} & \sqrt{2}c_{1123} & \sqrt{2}c_{1113} & \sqrt{2}c_{1112} \\ c_{1122} & c_{2222} & c_{2233} & \sqrt{2}c_{2223} & \sqrt{2}c_{2213} & \sqrt{2}c_{2212} \\ c_{1133} & c_{2233} & c_{3333} & \sqrt{2}c_{3323} & \sqrt{2}c_{3313} & \sqrt{2}c_{3312} \\ \sqrt{2}c_{1123} & \sqrt{2}c_{2223} & \sqrt{2}c_{3323} & 2c_{2323} & 2c_{2313} & 2c_{2312} \\ \sqrt{2}c_{1113} & \sqrt{2}c_{2213} & \sqrt{2}c_{3313} & 2c_{2313} & 2c_{1313} & 2c_{1312} \\ \sqrt{2}c_{1112} & \sqrt{2}c_{2212} & \sqrt{2}c_{3312} & 2c_{2312} & 2c_{1312} & 2c_{1212} \end{bmatrix} \begin{bmatrix} \varepsilon_{11} \\ \varepsilon_{22} \\ \varepsilon_{33} \\ \sqrt{2}\varepsilon_{23} \\ \sqrt{2}\varepsilon_{13} \\ \sqrt{2}\varepsilon_{12} \end{bmatrix}. \tag{1.5}$$

For a **transversely isotropic** tensor—within a system whose x_3 axis is parallel to the rotation symmetry axis—the components of C^{aniso} become

$$C^{\text{TI}} = \begin{bmatrix} c^{\text{TI}}_{1111} & c^{\text{TI}}_{1122} & c^{\text{TI}}_{1133} & 0 & 0 & 0 \\ c^{\text{TI}}_{1122} & c^{\text{TI}}_{1111} & c^{\text{TI}}_{1133} & 0 & 0 & 0 \\ c^{\text{TI}}_{1133} & c^{\text{TI}}_{1133} & c^{\text{TI}}_{3333} & 0 & 0 & 0 \\ 0 & 0 & 0 & 2c^{\text{TI}}_{2323} & 0 & 0 \\ 0 & 0 & 0 & 0 & 2c^{\text{TI}}_{2323} & 0 \\ 0 & 0 & 0 & 0 & 0 & c^{\text{TI}}_{1111} - c^{\text{TI}}_{1122} \end{bmatrix}. \tag{1.6}$$

A continuum whose symmetry group contains all orthogonal transformations is said to be **isotropic**. The arrangement of the zero entries and values of the nonzero entries remain the same for all orientations of an *orthonormal coordinate system*[4]. Comparatively, the elasticity matrix of an isotropic tensor has the simplest form of all tensors. For isotropy, the components of C^{aniso} become

$$C^{\text{iso}} = \begin{bmatrix} c^{\text{iso}}_{1111} & c^{\text{iso}}_{1111} - 2c^{\text{iso}}_{2323} & c^{\text{iso}}_{1111} - 2c^{\text{iso}}_{2323} & 0 & 0 & 0 \\ c^{\text{iso}}_{1111} - 2c^{\text{iso}}_{2323} & c^{\text{iso}}_{1111} & c^{\text{iso}}_{1111} - 2c^{\text{iso}}_{2323} & 0 & 0 & 0 \\ c^{\text{iso}}_{1111} - 2c^{\text{iso}}_{2323} & c^{\text{iso}}_{1111} - 2c^{\text{iso}}_{2323} & c^{\text{iso}}_{1111} & 0 & 0 & 0 \\ 0 & 0 & 0 & 2c^{\text{iso}}_{2323} & 0 & 0 \\ 0 & 0 & 0 & 0 & 2c^{\text{iso}}_{2323} & 0 \\ 0 & 0 & 0 & 0 & 0 & 2c^{\text{iso}}_{2323} \end{bmatrix}, \quad (1.7)$$

and expression (1.1) can be written as

$$\sigma_{ij} = (c_{1111} - 2c_{2323})\,\delta_{ij} \sum_{k=1}^{3} \varepsilon_{kk} + 2\,c_{2323}\,\varepsilon_{ij}\,, \qquad i,j \in \{1,2,3\}\,,$$

which is a simpler, two-parameter form of Hooke's Law.

[4]Normalized orthogonal coordinate system, where the planes meet at right angles to one another.

Chapter 2

Mathematical Norms as Physical Analogies

When computing an elasticity tensor based on empirical information, we must keep in mind that the symmetry class is a property of a Hookean solid, not a property of the physical material in question. A Hookean solid is a mathematical representation of the physical material. To consider a model for the mechanical properties of a material, it is useful to compute the distance between the obtained tensor and isotropy, as it provides a measure of accuracy for the model being used. Relations between such physical phenomena and mathematical structures are mediated by certain criteria, such as norms. The decision then lies in which norm is useful to compute this distance. In the following sections (2.1.1) and (2.1.2), we describe three norms—the Frobenius-36, the Frobenius-21 and operator norms—that are pertinent to use in such an approximation. In addition, we introduce a curve-fitting method, as it is also a relevant method to the approximations at hand.

2.1 Norms

To examine the "closeness" between the measured elasticity tensor and the reduced elasticity tensor, as discussed by Bos and Slawinski (2013) and by Danek et al. (2013, 2015), we consider possible norms of tensor (1.4).

A **norm** of a mathematical object is a quantity that in some possibly abstract sense, describes the length, size or magnitude of the object. It can be described as a function that takes a vector and gives it a real valued length. Norms exist for complex numbers, Gaussian integers, quaternions, vectors and matrices. One may be accustomed to a standard way of measuring Euclidean length, using the Euclidean norm (also known as the Frobenius norm), which can be expressed as

$$||x||_F = \sqrt{\sum_{i=1}^{m} |x_i|^2}\,. \tag{2.1}$$

However, the above expression is actually one type of norm and, in fact, there are many different "ways" of measuring this magnitude and, hence, there are many different types of norms—Frobenius norms, L_p norms, logarithmic norm, matrix norm, natural norm, polynomial norm, quaternion norm, Riemannian norm, spectral norm, and vector norm, just to name some.

In order for a function to be considered a norm, there are three axioms, or conditions, that the function must satisfy. These axioms are nonnegativity (also contains the sub-axiom of positivity), homogeneity, and the triangle inequality. They can be described as:

1. $||x|| \geq 0$, $||x|| = 0$ *if and only if* $x = 0$ — Nonegativity, Positivity

2. $||\alpha x|| = |\alpha| \, ||x||$ — Homogeneity

3. $||x + y|| \leq ||x|| + ||y||$ — Triangle Inequality

The first axiom states that the length of a given vector, x, must be greater than or equal to zero. Furthermore, its sub-axiom states that the length of a given vector, x, will equal zero only if x itself is equal to zero. The second axiom states that if a vector is scaled by some α, its length is equal to the absolute value of α multiplied by the length of x. The third axiom states that the length of the sum of two vectors, x and y, must be less than or equal to the length of x summed with the length of y. Mentioned in the given list of norms is the Frobenius norm.

Let us show how the Frobenius norm meets the three conditions required to be a norm. Recall axiom (1). Considering this axiom, one can say that $|x_i| \geq 0$, and squaring/square-rooting will not change the sign. Therefore, the only way that $||x|| = 0$ is if all $x_i = 0$. Secondly, consider axiom (2), the axiom of homogeneity. In linear algebra, an inner-product space is a vector space with an additional structure provided by an inner-product. This additional structure associates each pair of vectors in the space with a scalar quantity known as the inner product of the vectors. Therefore, for the second axiom, as it pertains to the Frobenius norms, we demonstrate the following proof:

Proof. Consider a vector x scaled by some magnitude, α:

$$\begin{aligned} ||\alpha x|| &= \sqrt{\alpha^2 \langle x; x \rangle} \\ &= |\alpha| \sqrt{\langle x; x \rangle} \\ &= |\alpha| \, ||x|| \, . \end{aligned}$$

□

Finally, considering the third axiom—the triangle inequality—and its relation to the Frobenius norms, one can prove its validity in the following way:

Proof. Consider two vectors, x and y:

$$\begin{aligned} ||x|| &= \sqrt{\langle x; x \rangle} \\ ||x + y||^2 &= \langle x + y; x + y \rangle \\ &\leq \langle x; x \rangle + \langle y; y \rangle + 2\sqrt{\langle x; x \rangle \langle y; y \rangle} \leq (||x|| + ||y||)^2 \, . \end{aligned}$$

□

As one can see from the three statements above, the Frobenius norms do, indeed, meet the criteria required of being a distance function.

In mathematics, a matrix norm extends the notion of a vector norm to matrices. If given an $m \times n$ matrix A_{mn} , one can think of it as a vector with mn entries, and apply any mn-dimensional vector norm. Any vector norm can be used as a matrix norm if you treat it as a large vector of numbers. Thus, the matrix norm is induced by the vector norm. If we think of A as an orthogonal transformation, then its norm is a measure of how much A can scale vectors. More specifically, let us focus on the group of L_p *norms*[1]. The induced matrix norm $||A||_p$ is defined by

[1]In mathematics, the L_p spaces are function spaces defined using a natural generalization of the p-norm for finite-dimensional vector spaces.

$$
\begin{aligned}
||A||_p &= \sup_{x \in C^n, x \neq 0} \frac{||Ax||_p}{||x||_p} \\
&= \sup_{x \in C^n, ||x||_p = 1} ||Ax||_p \\
&= \max_x \frac{||Ax||}{||x||} \\
&= \max_{||x||_{p=1}} ||Ax|| \,.
\end{aligned}
$$

If given a matrix A, when $p = 1$, the L_1 norm (or 1-norm) can be described as the maximum column sum of A, such that

$$
||A||_1 = \max_{1 \leq h \leq n} \sum_{i=1}^{n} |a_{ih}| \,.
$$

Similarly, when $p = \infty$ the L_∞ norm (or ∞-norm) can be described as the maximum row sum of a given matrix, A, such that

$$
||A||_\infty = \max_{1 \leq h \leq n} \sum_{j=1}^{n} |a_{hj}| \,.
$$

In the special case when $p = 2$, and one has square matrices ($m = n$), the induced matrix norm is the *spectral* norm, and also sometimes called the 2-norm or operator norm. The operator norm is defined on vector space $\mathbb{R}^n$ by

$$
||A||_2 = \lambda_1(A), \text{ the largest eigenvalue of } A \,. \tag{2.2}
$$

Operator $|| \cdot ||_2$ is induced by the Frobenius norms on $\mathbb{R}^n$ and, as a result, is a matrix norm. Generally, we are interested in a matrix norm that is invariant under orthogonal transformations. Consider the proof below. One can show that

Proof. Let $A = VUW$ be a singular value decomposition of A, in which V and W

are unitary, $U = \text{diag}(\lambda_1, \cdots, \lambda_n)$, and $\lambda_1 \geq \cdots \geq \lambda_n \geq 0$. We then have

$$\begin{aligned}
\max_{||x||_2=1} ||Ax||_2 &= \max_{||x||_2=1} ||VUW * x||_2 \\
&= \max_{||x||_2=1} ||UW * x||_2 \\
&= \max_{||Wy||_2=1} ||Uy||_2 \\
&= \max_{||y||_2=1} ||Uy||_2 \\
&\leq \max_{||y||_2=1} ||\lambda_1 y||_2 \\
&= \lambda_1 \max_{||y||_2=1} ||y||_2 \\
&= \lambda_1 \, .
\end{aligned} \tag{2.3}$$

□

Therefore, $||A||_2 = \lambda_1(A)$, the largest singular value of A.

2.1.1 Frobenius Norms

The Frobenius norm treats a matrix in $\mathbb{R}^{n \times n}$ as an Euclidean vector in $\mathbb{R}^{n^2}$. There are two types of Frobenius norms that we make use of in our study—the Frobenius-36 norm and the Frobenius-21 norm.

2.1.1.1 Frobenius-36 norm (F_{36})

In the case of a symmetric 6×6 matrix, where $C_{mn} = C_{nm}$, we can use the F_{36} norm:

$$||C||_{F_{36}} = \sqrt{\sum_{m=1}^{6} \sum_{n=1}^{6} C_{mn}^2} \, ,$$

which is the Frobenius norm using thirty-six components of expression (1.4), including their coefficients of $\sqrt{2}$ and 2.

2.1.1.2 Frobenius-21 norm (F_{21})

In light of $C_{mn} = C_{nm}$, the F_{36} norm allows for a weight-doubling for some off-diagonal entries. As a result, we might consider the F_{21} norm, which takes into account only the independent entries:

$$||C||_{F_{21}} = \sqrt{\sum_{m=1}^{6}\sum_{n=1}^{m} C_{mn}^2}\,.$$

As we can see, the above expression uses only the twenty-one independent components of expression (1.4), including their coefficients of $\sqrt{2}$ and 2.

2.1.2 Operator Norm

As discussed by Bos and Slawinski (2015), by treating a matrix as a vector, the Frobenius norms ignore the fact that a matrix is a representation of a linear map from $\mathbb{R}^n$ to $\mathbb{R}^n$. In view of equation (1.1), the elasticity tensor represents a linear map between the strain tensor, whose components can be expressed as a symmetric 3×3 matrix, $\varepsilon_{k\ell}$, and the stress tensor, whose components can be expressed as a symmetric 3×3 matrix, σ_{ij}. Furthering equation (2.2), the operator norm of the elasticity tensor considered as a mapping from $\mathbb{R}^{3\times3}$ to $\mathbb{R}^{3\times3}$, where both the stress and strain tensors are endowed with the F_{36} norm, is precisely the operator norm of matrix $C \in \mathbb{R}^{6\times6}$.

Given a norm on $\mathbb{R}^n$, the associated operator norm of matrix $A \in \mathbb{R}^{n\times n}$ is

$$||A|| := \max_{||x||=1} ||Ax||. \tag{2.4}$$

An example of such a norm is the Euclidean operator norm which—for symmetric matrices—becomes

$$||A||_2 := \max\{|\lambda| : \lambda \text{ an eigenvalue of A}\}. \tag{2.5}$$

The operator norm of an elasticity tensor—whose components in a given coordinate system can be expressed as a symmetric 6×6 matrix—is

$$||C||_\lambda = \max|\lambda_i| \tag{2.6}$$

where $\lambda_i \in \{\lambda_1, \cdots, \lambda_6\}$ is an eigenvalue of C.

2.2 Slowness Curve L_2 Fit

In a manner similar to the F_{36} norm, F_{21} norm and operator norm, the slowness-curve L_2 fit is used to find an isotropic counterpart of an anisotropic Hookean solid. However, in contrast to these norms, which rely on finding the smallest distance between tensors, the L_2 fit relies on finding the best fit of circles—according to a chosen criterion—to noncircular wavefronts.

When using this approach, in a manner similar to the operator norm, we do not invoke explicit expressions for the components of the closest elasticity tensor, but we examine the effect of these components on certain quantities. For the operator norm, this quantity consists of eigenvalues; for the slowness-curve fit, this quantity consists of wavefront slownesses.

The direct results of the norms are the components of the corresponding isotropic tensors, and the wavefront-slowness circles are their consequences. The direct result

of the slowness-curve fit are slowness circles, and the components of the corresponding isotropic tensor are their consequence.

The best fit, in the L_2 sense, is the radius, r , that minimizes

$$S = \sum_{i=1}^{n} (s_i - r_i)^2 \,, \tag{2.7}$$

where s_i are n discretized values along the slowness curve, and $s_i - r_i$ is measured in the radial direction. Hence, r is the radius of the slowness circle; it corresponds to isotropy, as isotropy is a spherical, two-parameter approximation.

Chapter 3

Tensor C and its Closest Symmetric Counterparts

3.1 Introduction

To study material symmetries, we wish to use the transformation of an orthonormal coordinate system in the $x_1x_2x_3$-space. A change of an orthonormal coordinate system in our three-dimensional space is given by

$$\hat{x} = Ax\,, \tag{3.1}$$

where $x = [x_1, x_2, x_3]^T$ and $\hat{x} = [\hat{x}_1, \hat{x}_2, \hat{x}_3]^T$ are the original and transformed coordinate systems, respectively, and A is the transformation matrix. Equation (3.1) is the matrix form of

$$\hat{x}_i = \sum_{j=1}^{3} a_{ij}x_j\,, \qquad i \in \{1, 2, 3\}\,.$$

We are interested in transformations that allow us to change the orientation of the continuum without deforming it. These transformations are distance-preserving transformations—rotations and reflections. They are represented by orthogonal matrices, that is, by square matrices given by

$$A = \begin{bmatrix} A_{11} & A_{12} & A_{13} \\ A_{21} & A_{22} & A_{23} \\ A_{31} & A_{32} & A_{33} \end{bmatrix}, \tag{3.2}$$

that satisfy the orthogonality condition, namely, $A^T A = I$, which is equivalent to $A^T = A^{-1}$, where T denotes transform.

There are eight classes of material symmetry. These classes, which range from low symmetry to high symmetry, are termed anisotropic, monoclinic, orthotropic, trigonal, tetragonal, cubic, transversely isotropic, and isotropic. For the purposes of this study, we will be focusing only on anisotropic, transversely isotropic, and isotropic symmetry classes. Their tensor forms are described in section (1.2.3), in expressions (1.4), (1.6), and (1.7), respectively.

Consider a trigonal continuum. Although the trigonal symmetry class is not prevalently used in this study, a special case of it is. It is a continuum whose symmetry group contains rotations about an axis by θ, where $\theta = \frac{2\pi}{3}$ and $\theta = \frac{4\pi}{3}$. To obtain the elasticity matrix for this continuum, we consider the orthogonal transformation that is represented by matrix (3.2) in the form given by

$$A_{x_3\theta} = \begin{bmatrix} \cos(\theta) & \sin(\theta) & 0 \\ -\sin(\theta) & \cos(\theta) & 0 \\ 0 & 0 & 1 \end{bmatrix}, \tag{3.3}$$

that corresponds to rotation by angle θ about the x_3 axis. Now consider another case. Suppose that a continuum is invariant with respect to a single rotation given by matrix (3.3), where θ is smaller than $\frac{\pi}{2}$. Consider, for example, $\theta = \frac{2\pi}{5}$, and, hence, assume that the symmetry group contains

$$A_{x_3\theta} = \begin{bmatrix} \cos(\frac{2\pi}{5}) & \sin(\frac{2\pi}{5}) & 0 \\ -\sin(\frac{2\pi}{5}) & \cos(\frac{2\pi}{5}) & 0 \\ 0 & 0 & 1 \end{bmatrix}. \tag{3.4}$$

Following condition (1.2), the elasticity matrix, C, satisfies the equation given by

$$C = M^T_{A_{x_3}\frac{2\pi}{5}} C M_{A_{x_3}\frac{2\pi}{5}}. \tag{3.5}$$

Equation (3.5) can be solved directly to give relations among the entries of C. The solution to condition (3.5) is the transversely isotropic tensor given by expression (1.6). [1]

In order to obtain such a tensor when given a generally anisotropic tensor, namely expression (1.4), we can analytically obtain components of the Frobenius-36 norm effective transversely isotropic tensor. They are (Moakher and Norris (2006), Bucataru and Slawinski (2009)):

[1] For further insight, refer to Slawinski (2015, page 162).

$$c^{\mathrm{TI}}_{1111} = \frac{1}{8}(3c_{1111} + 3c_{2222} + 2c_{1122} + 4c_{1212})\,, \tag{3.6}$$

$$c^{\mathrm{TI}}_{1122} = \frac{1}{8}(c_{1111} + c_{2222} + 6c_{1122} - 4c_{1212})\,, \tag{3.7}$$

$$c^{\mathrm{TI}}_{1133} = \frac{1}{2}(c_{1133} + c_{2233})\,, \tag{3.8}$$

$$c^{\mathrm{TI}}_{2323} = \frac{1}{2}(c_{2323} + c_{1313})\,, \tag{3.9}$$

$$c^{\mathrm{TI}}_{3333} = c_{3333}\,, \tag{3.10}$$

where $c_{ijk\ell}$ are the components of the generally anisotropic tensor (1.4). In these expressions we assume that both the generally anisotropic and transversely isotropic tensors are expressed with respect to the coordinate systems of the same orientation. No analytic form of the operator-norm effective tensor is known.

3.2 Tensor C

In this section, we investigate isotropic counterparts, of a given generally anisotropic tensor, for the three norms introduced in section 2.1. To consider a case that is pertinent to seismological studies, we use a transversely isotropic tensor derived from a generally anisotropic tensor obtained from the measurements of vertical seismic

profiling (VSP) by Dewangan and Grechka (2003),

$$C = \begin{bmatrix} 7.8195 & 3.4495 & 2.5667 & \sqrt{2}(0.1374) & \sqrt{2}(0.0558) & \sqrt{2}(0.1239) \\ 3.4495 & 8.1284 & 2.3589 & \sqrt{2}(0.0812) & \sqrt{2}(0.0735) & \sqrt{2}(0.1692) \\ 2.5667 & 2.3589 & 7.0908 & \sqrt{2}(-0.0092) & \sqrt{2}(0.0286) & \sqrt{2}(0.1655) \\ \sqrt{2}(0.1374) & \sqrt{2}(0.0812) & \sqrt{2}(-0.0092) & 2(1.6636) & 2(-0.0787) & 2(0.1053) \\ \sqrt{2}(0.0558) & \sqrt{2}(0.0735) & \sqrt{2}(0.0286) & 2(-0.0787) & 2(2.0660) & 2(-0.1517) \\ \sqrt{2}(0.1239) & \sqrt{2}(0.1692) & \sqrt{2}(0.1655) & 2(0.1053) & 2(-0.1517) & 2(2.4270) \end{bmatrix}. \tag{3.11}$$

Its components are density-scaled elasticity parameters with units of km^2/s^2. In other words, the Hookean solid in question is completely described by tensor (3.11).

3.3 Tensor C_a^{TI}

Let us consider a transversely isotropic tensor (Danek et al. 2013), which is the closest—in the F_{36} sense—counterpart of tensor (3.11),

$$C_a^{\mathrm{TI}} = \begin{bmatrix} 8.0641 & 3.3720 & 2.4588 & 0 & 0 & 0 \\ 3.3720 & 8.0641 & 2.4588 & 0 & 0 & 0 \\ 2.4588 & 2.4588 & 7.0817 & 0 & 0 & 0 \\ 0 & 0 & 0 & 2(1.8625) & 0 & 0 \\ 0 & 0 & 0 & 0 & 2(1.8625) & 0 \\ 0 & 0 & 0 & 0 & 0 & 2(2.3460) \end{bmatrix}. \tag{3.12}$$

Tensor (3.3) is obtained by minimizing the distance using expressions (3.6)-(3.10).

Isotropic tensors discussed herein are counterparts of this tensor. The slowness curves for tensor (3.12) and its isotropic counterpart circles are shown in Figure 3.1; these counterparts nearly coincide with each other.

One could use another norm to obtain a transversely isotropic tensor for the pur-

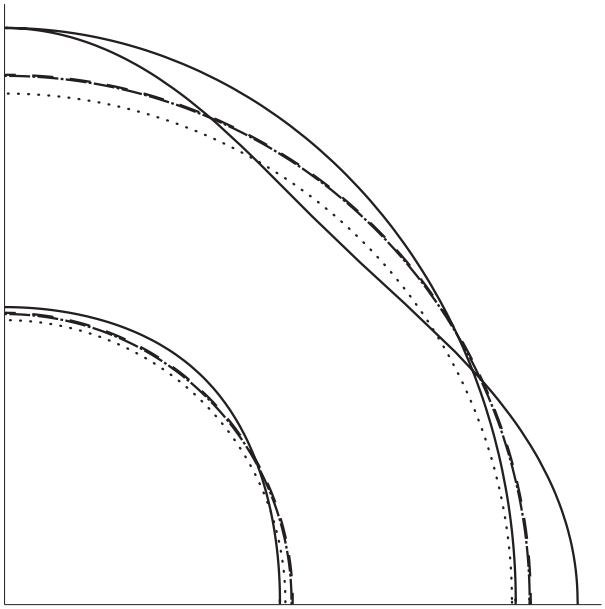

Figure 3.1: Slowness curves for tensor (3.12): solid lines represent the qP, qSV and SH waves; dashed lines represent the P and S waves according to F_{36} norm; dashed-dotted lines represent the P and S waves according to F_{21} norm; the results of these norms almost coincide; dotted lines represent the P and S waves according to λ norm.

pose of this study. Also—for the purpose of this study—one could use an anisotropic tensor to find its isotropic counterparts. We chose to consider the isotropic counterparts of a transversely isotropic tensor to be able to illustrate them graphically, as shown in Figures (4.3) and (4.4) in the next chapter, where we compare the norms used. The examination commencing from a generally anisotropic tensor is discussed by Danek et. al in 'Effects of norms on general Hookean solids for their isotropic counterparts.'

3.4 Tensor $C_a^{\mathbf{iso}}$

3.4.1 $C_a^{\mathbf{iso_{F_{36}}}}$

Let us consider the Frobenius norm using the thirty-six components (F_{36}). The analytical formulæ to calculate—from a generally anisotropic tensor—the two parameters of its closest isotropic tensor are given by Voigt (1910). From a transversely isotropic tensor, these parameters are

$$c_{1111}^{\mathrm{iso}_{F_{36}}} = \frac{1}{15}(8c_{1111}^{\mathrm{TI}} + 4c_{1133}^{\mathrm{TI}} + 8c_{2323}^{\mathrm{TI}} + 3c_{3333}^{\mathrm{TI}})$$

and

$$c_{2323}^{\mathrm{iso}_{F_{36}}} = \frac{1}{15}(c_{1111}^{\mathrm{TI}} - 2c_{1133}^{\mathrm{TI}} + 5c_{1212}^{\mathrm{TI}} + 6c_{2323}^{\mathrm{TI}} + c_{3333}^{\mathrm{TI}})\,.$$

Using the above formulæ, the closest isotropic counterpart of tensor (3.12) is

$$C_a^{\mathrm{iso}_{F_{36}}} = \begin{bmatrix} 7.3662 & 2.9484 & 2.9484 & 0 & 0 & 0 \\ 2.9484 & 7.3662 & 2.9484 & 0 & 0 & 0 \\ 2.9484 & 2.9484 & 7.3662 & 0 & 0 & 0 \\ 0 & 0 & 0 & 2(2.2089) & 0 & 0 \\ 0 & 0 & 0 & 0 & 2(2.2089) & 0 \\ 0 & 0 & 0 & 0 & 0 & 2(2.2089) \end{bmatrix}. \tag{3.13}$$

3.4.2 $C_a^{\mathbf{iso_{F_{21}}}}$

Let us consider the Frobenius norm using the twenty-one independent components (F_{21}). The analytical formulæ to calculate the two parameters of its closest isotropic tensor (Slawinski, 2016) are

$$c_{1111}^{\mathrm{iso}_{F_{21}}} = \frac{1}{9}(-c_{1122}^{\mathrm{TI}} + 2(3c_{2222}^{\mathrm{TI}} + c_{2233}^{\mathrm{TI}} + 2c_{2323}^{\mathrm{TI}} + c_{3333}^{\mathrm{TI}}))$$

and

$$c_{2323}^{\mathrm{iso}_{F_{21}}} = \frac{1}{18}(-5c_{1122}^{\mathrm{TI}} + 6c_{2222}^{\mathrm{TI}} - 2c_{2233}^{\mathrm{TI}} + 8c_{2323}^{\mathrm{TI}} + c_{3333}^{\mathrm{TI}})\,.$$

Similarly, we obtain

$$C_a^{\mathrm{iso}_{F_{21}}} = \begin{bmatrix} 7.4279 & 3.0716 & 3.0716 & 0 & 0 & 0 \\ 3.0716 & 7.4279 & 3.0716 & 0 & 0 & 0 \\ 3.0716 & 3.0716 & 7.4279 & 0 & 0 & 0 \\ 0 & 0 & 0 & 2(2.1781) & 0 & 0 \\ 0 & 0 & 0 & 0 & 2(2.1781) & 0 \\ 0 & 0 & 0 & 0 & 0 & 2(2.1781) \end{bmatrix}. \tag{3.14}$$

3.4.3 $C_a^{\mathrm{iso}_\lambda}$

Unlike the Frobenius norms, the operator norm has no analytical formulæ for $c_{1111}^{\mathrm{iso}_\lambda}$ and $c_{2323}^{\mathrm{iso}_\lambda}$. They must be obtained numerically. The largest eigenvalues are obtained using a standard numerical procedure of the Singular Value Decomposition and then optimized over a two-dimensional solution space using a similar procedure to the one described in Danek et al. (2013). For tensor (3.12), we obtain

$$C_a^{\mathrm{iso}_\lambda} = \begin{bmatrix} 7.7562 & 3.0053 & 3.0053 & 0 & 0 & 0 \\ 3.0053 & 7.7562 & 3.0053 & 0 & 0 & 0 \\ 3.0053 & 3.0053 & 7.7562 & 0 & 0 & 0 \\ 0 & 0 & 0 & 2(2.3755) & 0 & 0 \\ 0 & 0 & 0 & 0 & 2(2.3755) & 0 \\ 0 & 0 & 0 & 0 & 0 & 2(2.3755) \end{bmatrix}. \tag{3.15}$$

3.4.4 Distances Among Tensors

To gain insight into different isotropic counterparts of tensor (3.12), we calculate the F_{36} distance between tensors (3.13) and (3.15), which is 0.8993. The F_{36} distance

between tensors (3.12) and (3.13) is 1.8461 . The F_{36} distance between tensors (3.12) and (3.15) is 2.0535 , where we note that tensor (3.15) is the closest isotropic tensor according to the operator—not the F_{36}—norm. Thus, in spite of similarities between the isotropic tensors, the distance between them is large in comparison to their distances to tensor (3.12).

This is an illustration of abstractness of the concept of distances in the space of elasticity tensors. A concrete evaluation is provided by comparing the results obtained by minimizing these distances. Such results are tensors (3.13), (3.14), (3.15), and their wavefront-slowness circles in Figure 3.1. This figure illustrates a similarity among these circles, which is a realm in which the isotropic tensors can be compared.

Chapter 4

Comparison of Norms

When comparing tensors (3.13), (3.14) and (3.15), we see that the parameters of the closest isotropic tensor depend on the norm used. Given two anisotropic tensors, we might be interested to know which of them is closer to isotropy. For a given norm, a unique answer is obtained by a straightforward calculation. In general, for different norms, there is no absolute answer: the sequence in closeness to isotropy can be reversed between two tensors; it depends on the norms.

4.1 $\mathbf{F_{36}}$ versus $\mathbf{F_{21}}$

Using a numerical search based on a single random walk through a solution space with the target function being a difference between the minimized F_{21} distance and the maximized F_{36} distance, an elasticity tensor is generated that is further from isotropy than tensor (3.12) according to the F_{36} norm, but closer to isotropy than tensor (3.12) according to the F_{21} norm. The search results in a transversely isotropic

tensor, different from that of C_a^{TI}

$$C_{\mathrm{b}}^{\mathrm{TI}} = \begin{bmatrix} 7.3091 & 4.5882 & 2.9970 & 0 & 0 & 0 \\ 4.5882 & 7.3091 & 2.9970 & 0 & 0 & 0 \\ 2.9970 & 2.9970 & 6.6604 & 0 & 0 & 0 \\ 0 & 0 & 0 & 2(1.5631) & 0 & 0 \\ 0 & 0 & 0 & 0 & 2(1.5631) & 0 \\ 0 & 0 & 0 & 0 & 0 & 2(1.3605) \end{bmatrix}, \tag{4.1}$$

with its corresponding F_{36} and F_{21} isotropic counterparts,

$$C_{\mathrm{b}}^{\mathrm{iso}_{\mathrm{F}_{36}}} = \begin{bmatrix} 6.8631 & 3.6422 & 3.6422 & 0 & 0 & 0 \\ 3.6422 & 6.8631 & 3.6422 & 0 & 0 & 0 \\ 3.6422 & 3.6422 & 6.8631 & 0 & 0 & 0 \\ 0 & 0 & 0 & 2(1.6104) & 0 & 0 \\ 0 & 0 & 0 & 0 & 2(1.6104) & 0 \\ 0 & 0 & 0 & 0 & 0 & 2(1.6104) \end{bmatrix} \tag{4.2}$$

and

$$C_{\mathrm{b}}^{\mathrm{iso}_{\mathrm{F}_{21}}} = \begin{bmatrix} 6.9014 & 3.7188 & 3.7188 & 0 & 0 & 0 \\ 3.7188 & 6.9014 & 3.7188 & 0 & 0 & 0 \\ 3.7188 & 3.7188 & 6.9014 & 0 & 0 & 0 \\ 0 & 0 & 0 & 2(1.5913) & 0 & 0 \\ 0 & 0 & 0 & 0 & 2(1.5913) & 0 \\ 0 & 0 & 0 & 0 & 0 & 2(1.5913) \end{bmatrix}, \tag{4.3}$$

respectively.

The distances from $C_{\mathrm{a}}^{\mathrm{TI}}$ and $C_{\mathrm{b}}^{\mathrm{TI}}$ to isotropy—stated, respectively, in expressions (3.12) and (4.1)—using the F_{36} and F_{21} norms, are calculated using the following expressions

$$d_a = \left| ||C_a^{\mathrm{TI}}|| - ||C_a^{\mathrm{iso}}|| \right| \text{ and } d_b = \left| ||C_b^{\mathrm{TI}}|| - ||C_b^{\mathrm{iso}}|| \right|.$$

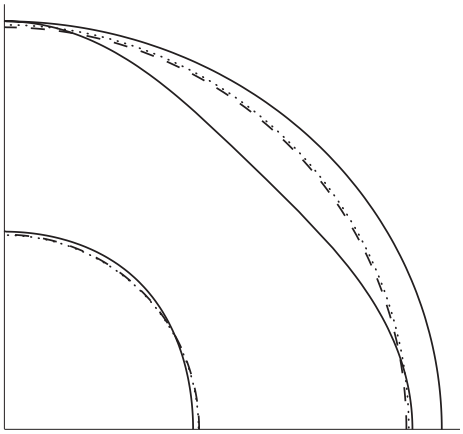

Figure 4.1: Slowness curves for tensor (4.1): solid lines represent the qP , qSV and SH waves; dashed lines represent the P and S waves according to F_{36} norm; dotted lines represent the P and S waves according to F_{21} norm.

From here, we obtain values where

$$d_{a_{21}} = 1.6372 > d_{b_{21}} = 1.5517\,,$$

$$d_{a_{36}} = 1.8460 < d_{b_{36}} = 2.0400\,.$$

The slowness curves for tensor (4.1) and its isotropic counterparts are shown in Figure 4.1.

4.2 F_{36} versus λ

The second comparison is between the F_{36} norm and the λ norm. We obtain

$$C_{bb}^{TI} = \begin{bmatrix} 6.8639 & 3.3046 & 2.8770 & 0 & 0 & 0 \\ 3.3046 & 6.8639 & 2.8770 & 0 & 0 & 0 \\ 2.8770 & 2.8770 & 8.3825 & 0 & 0 & 0 \\ 0 & 0 & 0 & 2(2.7744) & 0 & 0 \\ 0 & 0 & 0 & 0 & 2(2.7744) & 0 \\ 0 & 0 & 0 & 0 & 0 & 2(1.7797) \end{bmatrix}, \qquad (4.4)$$

which is further from isotropy according to the F_{36} norm and closer to isotropy according to the λ norm. Its isotropic counterparts in the sense of the F_{36} and λ norms are

$$C_{\mathrm{bb}}^{\mathrm{iso}_{\mathrm{F}_{36}}} = \begin{bmatrix} 7.5842 & 2.9125 & 2.9125 & 0 & 0 & 0 \\ 2.9125 & 7.5842 & 2.9125 & 0 & 0 & 0 \\ 2.9125 & 2.9125 & 7.5842 & 0 & 0 & 0 \\ 0 & 0 & 0 & 2(2.3358) & 0 & 0 \\ 0 & 0 & 0 & 0 & 2(2.3358) & 0 \\ 0 & 0 & 0 & 0 & 0 & 2(2.3358) \end{bmatrix} \tag{4.5}$$

and

$$C_{\mathrm{bb}}^{\mathrm{iso}_{\lambda}} = \begin{bmatrix} 7.4712 & 2.9171 & 2.9171 & 0 & 0 & 0 \\ 2.9171 & 7.4712 & 2.9171 & 0 & 0 & 0 \\ 2.9171 & 2.9171 & 7.4712 & 0 & 0 & 0 \\ 0 & 0 & 0 & 2(2.7704) & 0 & 0 \\ 0 & 0 & 0 & 0 & 2(2.7704) & 0 \\ 0 & 0 & 0 & 0 & 0 & 2(2.7704) \end{bmatrix}, \tag{4.6}$$

respectively. The distances to isotropy for $C_{\mathrm{a}}^{\mathrm{TI}}$ and $C_{\mathrm{bb}}^{\mathrm{TI}}$, using the F_{36} and λ norms, are

$$\mathrm{d}_{\mathrm{a}_{36}} = 1.8460 < \mathrm{d}_{\mathrm{bb}_{36}} = 2.1825\,,$$

$$\mathrm{d}_{\mathrm{a}_{\lambda}} = 1.0259 > \mathrm{d}_{\mathrm{bb}_{\lambda}} = 0.9947\,.$$

The slowness curves for tensor (4.4) and its isotropic counterparts are shown in Figure 4.2.

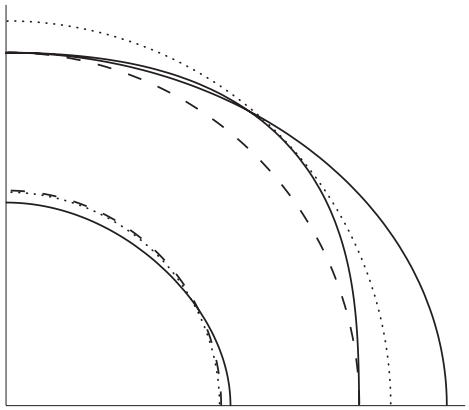

Figure 4.2: Slowness curves for tensor (4.4): solid lines represent the qP , qSV and SH waves; dotted lines represent its P and S waves according to F_{36} norm; dashed lines represent its P and S waves according to λ norm.

4.3 F_{21} versus λ

The third comparison is between the F_{21} norm and the λ norm. The resulting tensor is

$$C^{\mathrm{TI}}_{\mathrm{bbb}} = \begin{bmatrix} 4.5706 & 2.6852 & 2.9075 & 0 & 0 & 0 \\ 2.6852 & 4.5706 & 2.9075 & 0 & 0 & 0 \\ 2.9075 & 2.9075 & 5.2705 & 0 & 0 & 0 \\ 0 & 0 & 0 & 2(1.9145) & 0 & 0 \\ 0 & 0 & 0 & 0 & 2(1.9145) & 0 \\ 0 & 0 & 0 & 0 & 0 & 2(0.9427) \end{bmatrix}, \qquad (4.7)$$

with isotropic counterparts according to the F_{21} norm and the λ norm,

$$C^{\mathrm{iso}_{\mathrm{F}_{21}}}_{\mathrm{bbb}} = \begin{bmatrix} 5.2074 & 2.4297 & 2.4297 & 0 & 0 & 0 \\ 2.4297 & 5.2074 & 2.4297 & 0 & 0 & 0 \\ 2.4297 & 2.4297 & 5.2074 & 0 & 0 & 0 \\ 0 & 0 & 0 & 2(1.3889) & 0 & 0 \\ 0 & 0 & 0 & 0 & 2(1.3889) & 0 \\ 0 & 0 & 0 & 0 & 0 & 2(1.3889) \end{bmatrix} \qquad (4.8)$$

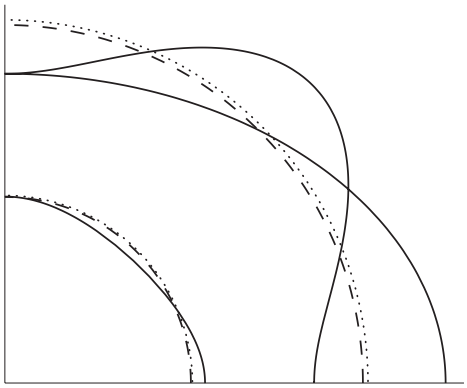

Figure 4.3: Slowness curves for tensor (4.7): solid lines represent the qP , qSV and SH waves; dotted lines represent its P and S waves according to F_{21} norm; dashed lines represent its P and S waves according to λ norm.

and

$$C_{\mathrm{bbb}}^{\mathrm{iso}_\lambda} = \begin{bmatrix} 5.2926 & 2.4354 & 2.4354 & 0 & 0 & 0 \\ 2.4354 & 5.2926 & 2.4354 & 0 & 0 & 0 \\ 2.4354 & 2.4354 & 5.2926 & 0 & 0 & 0 \\ 0 & 0 & 0 & 2(1.4286) & 0 & 0 \\ 0 & 0 & 0 & 0 & 2(1.4286) & 0 \\ 0 & 0 & 0 & 0 & 0 & 2(1.4286) \end{bmatrix}, \tag{4.9}$$

respectively. The distances to isotropy for both $C_{\mathrm{a}}^{\mathrm{TI}}$ and $C_{\mathrm{bbb}}^{\mathrm{TI}}$ using the F_{21} and λ norms are

$$\mathrm{d}_{\mathrm{a}_{21}} = 1.6372 < \mathrm{d}_{\mathrm{bbb}_{21}} = 2.0842\,,$$

$$\mathrm{d}_{\mathrm{a}_\lambda} = 1.0259 > \mathrm{d}_{\mathrm{bbb}_\lambda} = 0.9719\,.$$

The slowness curves for tensor (4.7) and its isotropic counterparts are shown in Figure 4.3.

4.4 Slowness Curve L_2 Fit

Considering tensor (3.12) and applying a minimization for the qP wave, using formula (2.7), we find $\mathrm{S} = 0.0886$ with $\mathrm{r} = 0.3770$. Following the same procedure for the qSV and SH waves, we find $\mathrm{S} = 0.2973$, with $\mathrm{r} = 0.6832$, and $\mathrm{S} = 0.2169$, with $\mathrm{r} = 0.6831$, respectively. Combining these results, we obtain $\mathrm{S} = 0.6029$, with $\mathrm{r_P} = 0.3770$ and $\mathrm{r_S} = 0.6831$, which are the slownesses of the P and S waves, respectively. Note that—since the slowness curves of the qP waves are detached from the curves for the qSV and SH waves—the value of r for the P waves does not change by combining the results.

Since $v_P = \sqrt{c_{1111}}$ and $v_S = \sqrt{c_{2323}}$ are the P-wave and S-wave speeds, respectively, it follows that $c_{1111} = 1/r_P^2$ and $c_{2323} = 1/r_S^2$. Hence, we obtain

$$C_a^{\mathrm{iso}_{L_2}} = \begin{bmatrix} 7.0341 & 2.7485 & 2.7485 & 0 & 0 & 0 \\ 2.7485 & 7.0341 & 2.7485 & 0 & 0 & 0 \\ 2.7485 & 2.7485 & 7.0341 & 0 & 0 & 0 \\ 0 & 0 & 0 & 2(2.1428) & 0 & 0 \\ 0 & 0 & 0 & 0 & 2(2.1428) & 0 \\ 0 & 0 & 0 & 0 & 0 & 2(2.1428) \end{bmatrix}. \tag{4.10}$$

The slowness curves for tensor (4.10) and its isotropic counterparts are shown in Figure 4.4.

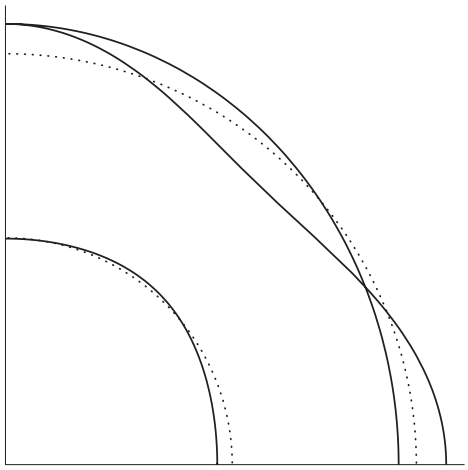

Figure 4.4: Slowness curves for tensor (4.10): solid lines represent the qP , qSV and SH waves; dotted lines represent its P and S waves according to the slowness-curve L_2 fit.

Chapter 5

Error Propagation

Components of an anisotropic tensor obtained from experimental measurements exhibit uncertainties due to measurement errors. These uncertainties are carried to its symmetric counterparts. In-depth studies of probability laws for the stiffness components was a subject of a paper by Guilleminot and Soize (2013). In general, the off-diagonal terms may be safely assumed to be a Gaussian, but the diagonal ones are the Gamma-random variables. The statistical dependence structure for the six strongest symmetry classes, namely, isotropic, transversely isotropic, cubic, tetragonal, trigonal and orthotropic, is presented in Table (1) of Guilleminot and Soize (2013). From the practical point of view of seismic observations, this problem was analyzed by Rusmanugroho and McMechan (2012). In this case, normality—expressed as a large-shape parameter of the Gamma variables—and the independence assumptions are good analogies for real observations, even though certain components, such as c_{1212} and c_{1223} , have the values of the crosscorrelation matrix significantly higher than others, due to the relation between their horizontal and vertical stress, and horizontally polar-

ized strain. These assumptions, namely independence of components and normality of their distributions, were the gist of the approach presented in Danek et al. (2015). They are also—at least partially—required to obtain matrix (5.1) through numerical simulations performed by Dewangan and Grechka (2003). Let us examine the error propagation between the transversely isotropic tensor and its isotropic counterparts. Apart from inferring the stability of these counterparts, such an examination allows us to generalize our conclusions to a range of tensors whose values are pertinent to seismological studies. Even though our conclusions stem from a single transversely isotropic tensor, the perturbation of it components is akin to considering a multitude of such tensors. The standard deviations of components of tensor (3.11) (Grechka, pers. comm., 2007) are

$$\pm \begin{bmatrix} 0.1656 & 0.1122 & 0.1216 & 0.1176 & 0.0774 & 0.0741 \\ 0.1122 & 0.1862 & 0.1551 & 0.0797 & 0.1137 & 0.0832 \\ 0.1216 & 0.1551 & 0.1439 & 0.0856 & 0.0662 & 0.1010 \\ 0.1176 & 0.0797 & 0.0856 & 0.0714 & 0.0496 & 0.0542 \\ 0.0774 & 0.1137 & 0.0662 & 0.0496 & 0.0626 & 0.0621 \\ 0.0741 & 0.0832 & 0.1010 & 0.0542 & 0.0621 & 0.0802 \end{bmatrix}. \tag{5.1}$$

Considering these standard deviations, we view the parameters of the effective tensors not as specific values but as ranges within which lie the best-fit values. These values do not constitute components of a tensor. Hence, they are valid only in the coordinate system of measurements, since rotations are not allowed. Thus, to consider error propagation from tensor (3.11) to tensor (3.12), with tensor (3.12) being the F_{36} closest TI counterpart, there is a need for a simulation. Probability distributions of the values of the components of tensor (3.12)—obtained by a Monte-Carlo simulation (Danek et al. 2013)—are shown in Figures 5.1a, 5.1b, 5.1c, 5.2, 5.3. Different

histograms have different horizontal scales. The probability distributions of the two

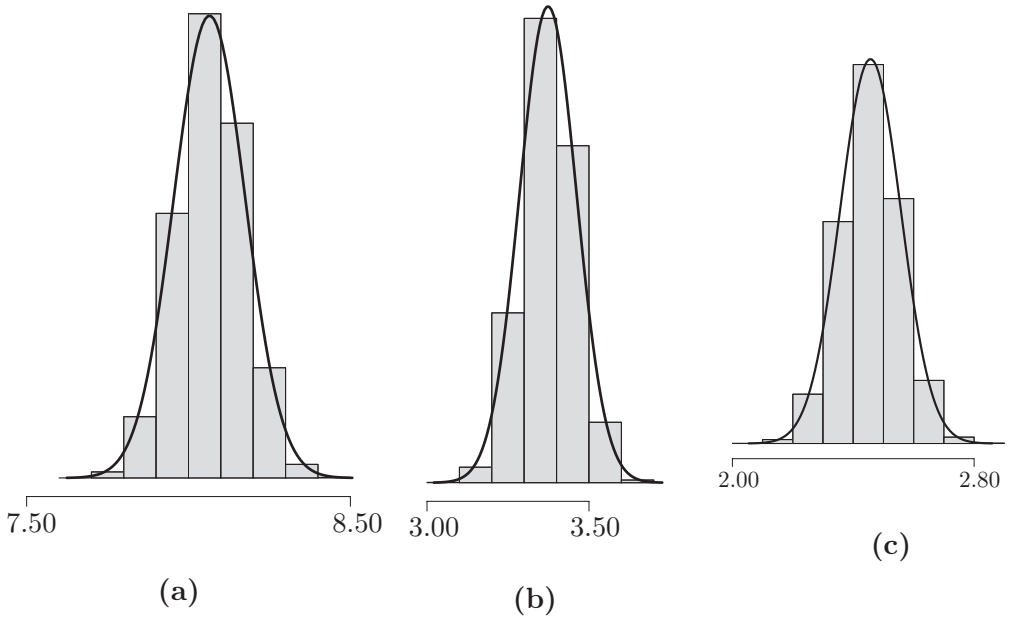

Figure 5.1: Elasticity parameters of tensor (3.12); c_{1111} depicted in subfigure (5.1a), c_{1122} depicted in subfigure (5.1b), c_{1133} depicted in subfigure (5.1c).

parameters for its isotropic F_{36} counterpart are obtained in the same manner and shown in Figure 5.4. Their mean values are given in tensor (3.13). The probability distributions of parameters for its F_{21} counterpart are also shown in Figure 5.4, as well are the probability distributions of parameters for its λ counterpart.

Performing a simple error-propagation analysis, we observe that—for Frobenius norms—probability distributions of the corresponding parameters are very similar to one another. For the operator norm, however, the c_{2323} distributions differ significantly. This result might be a consequence of the properties of the operator norm, where only the largest among six eigenvalues is taken into consideration.

Let us consider the highest symmetry—isotropy—for which the effective tensor

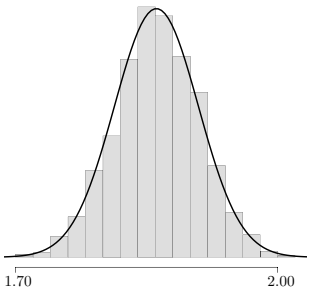

Figure 5.2: Elasticity parameter c_{2323} of tensor (3.12)

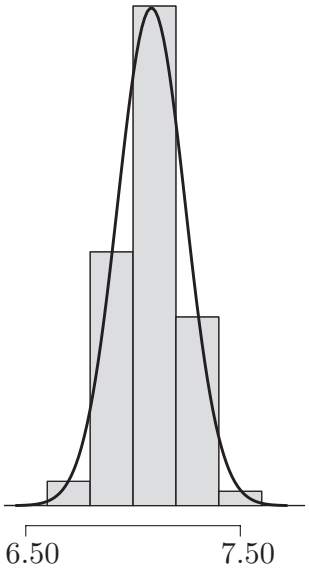

Figure 5.3: Elasticity parameter c_{3333} of tensor (3.12)

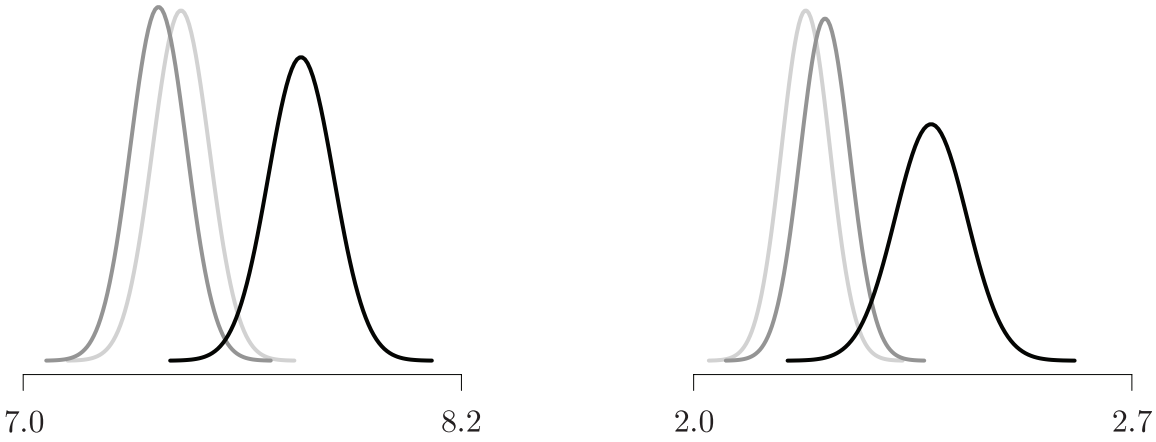

Figure 5.4: Elasticity parameters c_{1111} (left panel) and c_{2323} (right panel) of F_{21} (light grey), F_{36} (dark grey) and λ (black) isotropic counterparts of tensor (3.12)

is independent of orientation, and—unlike for other symmetry classes—for all orientations, all $c^{\text{iso}}_{ijk\ell} = 0$, except $c^{\text{iso}}_{1111} = c^{\text{iso}}_{2222} = c^{\text{iso}}_{3333}$, $c^{\text{iso}}_{1122} = c^{\text{iso}}_{1133} = c^{\text{iso}}_{2233}$ and $c^{\text{iso}}_{1212} = c^{\text{iso}}_{1313} = c^{\text{iso}}_{2323}$. Using the twenty-one parameters obtained by Dewangan and

Grechka (2003), we can find the closest isotropic tensor by invoking Voigt's (1910) formulae. The question, however, remains—is it a good enough analogy for the physical material being considered? To investigate, let us consider entries that are zero. The entry at the first row and fourth column is 0.1374 ± 0.1176, which means that zero is more than one standard deviation away. It follows from properties of the Gaussian distribution that probability of the required zero is less than 30%. For the entry at the second row and the sixth column we have 0.1692 ± 0.0832, where the required zero is more than two standard deviations away and gives a probability of less than 5%. Therefore, conditions for isotropy are not likely to be satisfied.

Since, in seismology, we use remote measurements, such as geophones on the surface responding to interior disturbances, the inferences between the measurements and the properties of the interior must be mediated by a theory. For seismology, this theory is continuum mechanics. Unfortunately, seismologists are limited to having an intermediate step between measurements and information about properties of the materials of interest. When inferring material properties from mathematical models, the best we can do is achieve consistency between observations and model predictions.

The focus of this paper entails three major points. First, anisotropy considered in the context of seismic measurements is a mathematical analogy for physical properties of materials. It deals directly with the symmetry of tensors and only indirectly with material properties of rocks. Second, the interpretation begins with the choice of an analogy, where the choice depends on the concept of sufficient accuracy with which a symmetric tensor represents the generally anisotropic one at hand. Finally, once the 'best-fit' analogy is decided upon, there are many physical situations that can account for that analogy. Anisotropy of a Hookean solid implies, analogically, a directional

pattern within a material, as opposed to a random arrangement. However, it does not provide explicit information about the causes for a given pattern or, in contrast, its absence. Transverse isotropy, for example, might be an analogy for parallel layers in a sedimentary basin or for the preferred orientation of olivine crystals in the Earth's mantle.

Therefore, the relations between anisotropy and fractures, while containing insights into material properties, must be applied with awareness of their limitations. There should be an inquiry into criteria for the choice of a model. For example, is the model with the transverse isotropy, whose symmetry axis is vertical, imposed beforehand and, if so, have the observations been forced into a model that is not the optimal choice? In general, many physical scenarios can be proposed to accommodate a given model and, in contrast, many models can be proposed to accommodate experimental data, particularly, if errors are taken into account. The awareness of the necessity for a theory to mediate between measurements and interpretations—and, hence, the unavoidable presence of abstract concepts, such as the symmetry of tensors for analysis of physical properties, such as fractures—is crucial for applied geophysics, as it is for any general theory to interpret or predict physical phenomena.

Chapter 6

Relation Between Mathematical and Physical Models

6.1 Stability Conditions

When mathematically modeling physical phenomena, stability conditions play an important role. They pertain to the necessity for a theory to mediate between measurements and interpretations and, as a result, are crucial to analogies representing physical media.

6.1.1 Physical Motivation

The strain-energy function is formulated in terms of parameters $c_{ijk\ell}$, where $i, j, k, \ell \in \{1, 2, 3\}$. This function provides the sole fundamental constraints on these parameters. These constraints are called stability conditions since they constitute a mathematical statement of the fact that it is necessary to expend energy to deform

a material. In other words, if energy is not expended, the material remains stable in its undeformed state. As a result, the strain-energy function of an undeformed continuum is zero. Therefore, since energy is a positive quantity, the strain-energy function must be a positive quantity that disappears only in the undeformed state of the continuum.

6.1.2 Mathematical Analogy

In a mathematical sense, the stability conditions are equivalent to the positive-definiteness of the elasticity matrix. To formulate the conditions of positive-definiteness of the elasticity matrix, we can use one of the following theorems from linear algebra:

Theorem 2. *A real symmetric matrix is positive-definite if and only if the determinants of all its leading principal minors, including the determinant of the matrix itself, are positive.*

or

Theorem 3. *A real symmetric matrix is positive-definite if and only if all its eigenvalues are positive.*

Since the matrix in question, (1.4), is symmetric, the stability conditions can be conveniently formulated based on Theorems (2) and (3). Among these conditions we find that

$$c_{ijij} > 0, \qquad i, j \in \{1, ..., 3\}, \tag{6.1}$$

which implies that all the main-diagonal entries of the elasticity matrix must be positive.

Consider matrix (1.6). The stability conditions require that matrix (1.6) be positive-definite. Recalling equations (6.1), we obtain

$$c_{1111} > 0\,, \tag{6.2}$$

$$c_{3333} > 0\,, \tag{6.3}$$

$$c_{2323} > 0\,, \tag{6.4}$$

$$c_{1111} > c_{1122}\,. \tag{6.5}$$

We notice that matrix (1.6) is a direct sum of two submatrices given by

$$C_1 = \begin{bmatrix} c_{1111} & c_{1122} & c_{1133} \\ c_{1122} & c_{1111} & c_{1133} \\ c_{1133} & c_{1133} & c_{3333} \end{bmatrix}\,, \tag{6.6}$$

and

$$C_2 = \begin{bmatrix} c_{2323} & 0 & 0 \\ 0 & c_{2323} & 0 \\ 0 & 0 & \frac{c_{1111}-c_{1122}}{2} \end{bmatrix}\,. \tag{6.7}$$

Conditions (6.4) and (6.5) ensure that matrix C_2 is positive-definite. In view of condition (6.2), the remaining conditions for the positive-definiteness of matrix C_1 are

$$\det \begin{bmatrix} c_{111} & c_{1122} \\ c_{1122} & c_{1111} \end{bmatrix} > 0\,, \tag{6.8}$$

and

$$\det \begin{bmatrix} c_{1111} & c_{1122} & c_{1133} \\ c_{1122} & c_{1111} & c_{1133} \\ c_{1133} & c_{1133} & c_{3333} \end{bmatrix} > 0\,. \tag{6.9}$$

The condition resulting from determinant (6.8) is

$$c_{1111} > |c_{1122}|\,, \tag{6.10}$$

while the condition resulting from determinant (6.9) is

$$c_{3333}(c_{1111} - c_{1122})(c_{1111} + c_{1122}) > 2c_{1133}^2(c_{1111} - c_{1122})\,. \tag{6.11}$$

In view of expression (6.5), we can rewrite the latter condition as

$$c_{3333}(c_{1111} + c_{1122}) > 2c_{1133}^2\,. \tag{6.12}$$

Also, in view of condition (6.3), we have $c_{1111} + c_{1122} > 0$. Consequently, condition (6.10) follows from conditions (6.3), (6.5) and (6.12). Thus, all the stability conditions for a transversely isotropic continuum are given by expressions (6.2), (6.3), (6.4), (6.5) and (6.12) (Slawinski, 2015). In addition, it is important to note that all transversely isotropic tensors used in this study—(3.12), (4.1), (4.4), and (4.7)—satisfy the stability conditions and, thus, are good mathematical analogies.

6.2 Strength of Anisotropy

Elasticity theory opens an avenue that allows for applications to problems in petroleum geophysics. In doing so, the elastic medium in question is assumed to be isotropic. However, most crustal rocks are found to be anisotropic. Consequently,

there is an inconsistency between practice and reality. We, however, still accept the existence of this inconsistency due to the fact that, in vertical reflection profiling, the most commonly occurring type of anisotropy—transverse isotropy—can be mistaken for isotropy as a result of its disguised angular dependence. In addition to that, the mathematical expressions used in representing anisotropic wave propagation can be cumbersome. However, in most cases that are of interest to geophysicists, the anisotropy is weak—10% to 20% (Thomsen, 1986). As a result we can, satisfactorily, simplify equations considerably.

In Thomsen's 1986 study on weak elastic anisotropy, he shows that the relation given in expression (1.1) may be used in the equation of motion, which yields a wave equation. This wave equation gives three independent solutions for each direction of wave propagation—one quasi-longitudinal, one transverse, and one quasi-transverse. Daley and Hron (1977) offer expressions to model the three phase velocities. They can be expressed as

$$\begin{aligned}
\rho v_P^2(\theta) &= \frac{1}{2}[c_{3333} + c_{2323} + (c_{1111} - c_{3333})\sin^2\theta + D(\theta)]\,, \\
\rho v_{SV}^2(\theta) &= \frac{1}{2}[c_{3333} + c_{2323} + (c_{1111} - c_{3333})\sin^2\theta - D(\theta)]\,, \\
\rho v_{SH}^2(\theta) &= c_{1212}\sin^2\theta + c_{2323}\cos^2\theta\,,
\end{aligned}$$

where ρ is density and θ is a phase angle between the wavefront normal and the vertical axis, and $D(\theta)$ can be described as

$$\begin{aligned}
D(\theta) = \{&c_{3333} - c_{2323}^2 + 2[2(c_{1133} + c_{2323})^2 - (c_{3333} - c_{2323})(c_{1111} + c_{3333} - 2c_{2323}]\sin^2\theta \\
&+ [(c_{1111} + c_{3333} - 2c_{2323})^2 - 4(c_{1133} + c_{2323})^2]\sin^4\theta\}^{\frac{1}{2}}\,.
\end{aligned} \tag{6.13}$$

The above equations involve five elastic moduli. It may be useful to recast those equations using notation involving only two elastic moduli which would be, equivalently, vertical $P-$wave and $S-$wave velocities, plus three measures of anisotropy. These three anisotropies should be appropriate combinations of elastic moduli which (1) are nondimensional; (2) simplify the above equations; and (3) reduce to zero in the case of isotropy, so that materials with values of $\ll 1$ of anisotropy may be considered to be weakly anisotropic (Thomsen, 1986).

Tensors (3.12), (4.1), (4.4) and (4.7) exhibit the strength of anisotropy that is consistent with cases of interest to geophysicists. To show this consistency, we calculate the Thomsen (1986) parameters,

$$\begin{aligned}
\alpha &= \sqrt{c^{\mathrm{TI}}_{3333}}\,, \\
\beta &= \sqrt{c^{\mathrm{TI}}_{2323}}\,, \\
\gamma &= \frac{c^{\mathrm{TI}}_{1212} - c^{\mathrm{TI}}_{2323}}{2c^{\mathrm{TI}}_{2323}}\,, \\
\delta &= \frac{(c^{\mathrm{TI}}_{1133} + c^{\mathrm{TI}}_{2323})^2 - (c^{\mathrm{TI}}_{3333} - c^{\mathrm{TI}}_{2323})^2}{2c^{\mathrm{TI}}_{3333}(c^{\mathrm{TI}}_{3333} - c^{\mathrm{TI}}_{2323})}\,, \\
\epsilon &= \frac{c^{\mathrm{TI}}_{1111} - c^{\mathrm{TI}}_{3333}}{2c^{\mathrm{TI}}_{3333}}\,.
\end{aligned}$$

As said above, the first two of the parameters, α and β, are measures of vertical P-wave and S-wave velocities, respectively. The last three of the parameters, γ, δ, and ε, are three measures of anisotropy. The values of these parameters for tensors (3.12), (4.1), (4.4) and (4.7) are shown in Table 6.1. Comparing results of this table to data of Auld (1973) and Thomsen (1986), we see that these tensors can represent common geological materials, and are good mathematical analogies for physical phenomena.

Table 6.1: Thomsen parameters for tensors (3.12), (4.1), (4.4) and (4.7)

Tensor	α	β	γ	δ	ε
C_a^{TI}	2.6612	1.2986	0.1956	-0.1561	0.0694
C_b^{TI}	2.5808	1.2503	-0.6483	-0.0764	0.0487
C_{bb}^{TI}	2.2958	1.3837	-0.2538	0.3389	-0.6640
C_{bbb}^{TI}	2.8953	1.6657	-0.1793	0.0052	-0.0906

Discussions and conclusions

In Section 2.1, we consider several types of norms, and later we use them in Chapter 3 for obtaining—for a transversely anisotropic tensor—its closest isotropic counterpart. We examine the Frobenius norms and the operator norm. In Section 2.2, we consider the slowness-curve L_2 fit to obtain such a counterpart, and implement in Section 4.4.

As shown in Sections 4.1, 4.2 and 4.3, given tensor (3.12), we can find another transversely isotropic tensor—representative of common geological materials—such that one of them is closer to isotropy according to one norm and the other closer to isotropy according to another norm. At first sight, such a result might emphasize the importance of the choice of a norm.

However, in view of Chapter 5, we conclude that the results of the three norms and the slowness-curve fit are so similar to each other that their corresponding values might be indistinguishable in the context of measurement errors, perhaps with the exception of the operator norm for c_{2323}, as discussed on page 35. Thus, the choice of the norm might be of secondary importance. Pragmatically, for a tensor obtained from seismic measurements, we might choose a Frobenius norm, since it offers analytical formulæ to obtain an isotropic counterpart. Both Frobenius norms result in similar

effective isotropic tensors, since they differ only by a weight doubling of the off-diagonal components, whose values are small. Also, in view of this similarity, the preference of norms used to measure closeness to isotropy for the pairs of tensors discussed in Chapter 4 might yield results that are indistinguishable from that of other norms.

Performing an error propagation, we observe that–for Frobenius norms–probability distributions of the corresponding parameters are very similar to one another. For the operator norm, however, the c_{2323} distributions differ more significantly. This result might be a consequence of the properties of the operator norm, where only the largest among six eigenvalues is taken into consideration.

Therefore, the generally anisotropic tensor obtained from physical measurements, is approximated to its closest effective isotropic tensor. The distance between these two tensors is commonly measured using the Frobenius-36 norm. This thesis entails an exploration of distance results of other norms—the Frobenius-21 and operator norms—as well as a slowness-curve L_2 fit. Such comparisons result in solutions and probability distributions that are very similar to one another. As a result, depending on criteria, one may choose to use one norm over another.

To ensure a realistic approach, Thomsen's parameters are calculated based on the four transversely isotropic tensors (3.12), (4.1), (4.4), (4.7) that are generated. They offer practical, numerical values for both the vertical P-wave and S-wave velocities, as well as the three measures of anisotropy. The transversely isotropic tensors satisfy the stability conditions described in Chapter 6 and exhibit weak anisotropy, according to Thomsen's parameters, thus providing adequate mathematical models for physical phenomena.

Moreover, we wish to state that a statistical study of reducing a generally anisotropic elasticity tensor to its counterparts of higher symmetry as a function of different norms is an interesting problem, but beyond the scope of this thesis. In this study, we examine consequences of the choice of a norm in reducing a typical tensor obtained from seismic measurements, subject to experimental errors, to its isotropic counterparts. Examples of tensors and the behaviour of their norms illustrated herein are insightful for both theoretical and empirical aspects of seismology.

Bibliography

Arsingy, V., Ayache, N., Fillard, P., Pennec, X., Log-Euclidean metrics for fast and simple calculus on diffusion tensors, *J. Mag. Res. in Med.,* **1**, 2–6, 2006.

Auld, B.A., *Acoustic Fields and Waves in Solids, Vol. 1*, Florida: Kreiger Publishing, 1978.

Backus, G.E., Long-wave elastic anisotropy produced by horizontal layering, *J. Geophys. Res.,* **67**, 11, 1962.

Bos, L., Slawinski, M.A., 2-norm effective isotropic Hookean solids, *J. Elast.*, **120**, 1, 1–22, 2014.

Bucataru, I., Slawinski, M.A., Invariant properties for finding distance in space of elasticity tensors, *J. Elast.*, **94**(2), 97-114, 2009.

Crampin, S. The basis for earthquake prediction, *J. Geophys.J.R.astr.Soc.*, **91**, 331-347, 1987.

Daley, P.F. and Hron, F., Reflection and transmission coefficients for transversely isotropic media: Bull. Seism. Soc. Am., **67**, 661–675, 1977.

Danek, T., Kochetov, M., Slawinski, M.A., Effective elasticity tensors in the context of random errors, *J. Elast.*, **121**, 1, 4, 2015.

Danek, T., Kochetov, M., Slawinski, M.A., Uncertainty analysis of effective elasticity tensors using quaternion-based global optimization and Monte-Carlo method, *Q. J. Mech. Appl. Math.*, **66**, 2, 2013.

Danek, T., Noseworthy, A., Slawinski, M.A., Effects of norms on general Hookean solids for their isotropic counterparts, *Dolomites Research Notes on Approximation*, **11**, 15-28, 2018.

Danek, T., Slawinski, M.A., On effective transversely isotropic elasticity tensors of Frobenius and L_2 operator norms, 2014.

Dewangan, P., Grechka, V., Inversion of multicomponent, multiazimuth walkaway VSP data for the stiffness tensor, *Geophys.*, **68**, 1022-1031, 2003.

Gazis, D.C., Tadjbakhsh, I., Toupin, R.A., The elastic tensor of given symmetry nearest to an anisotropic elastic tensor, *Acta. Cryst.*, **16**, 917, 1963.

Guilleminot, J., Soize, C., On the statistical dependence for the components of random elasticity tensors exhibiting material symmetry properties, *J. Elasticity*, **111**, 109–130, 2013.

Horn, Roger A., Johnson, Charles R., Norms for vectors and matrices. *Matrix Analysis*, 2nd Ed., (pp. 340–342). Cambridge: Cambridge University Press, 2013.

Kochetov, M., Slawinski, M.A., On obtaining effective transversely isotropic elasticity tensors, *J. Elas*, **94**, 1–13, 2009.

Lancaster, P., Tismenetsky, M., Norms and bounds for eigenvalues. *The Theory of Matrices*, (pp. 358–367). California: Academic Press, 1985.

Moakher, M., Norris, A.N., The closest elastic tensor of arbitrary symmetry to an elasticity tensor of lower symmetry, *J. Elas*, **85**, 215–263, 2006.

Norris, A.N., The isotropic material closest to a given anisotropic material, *J. Mech.*

Materials Struct., **1**, 2, 223–238, 2006.

Rusmanugroho, H., McMechan, G., 3D 9C seismic modeling and inversion of Weyburn Field data, *Geophysics*, **77**, 4, 161-173, 2012.

Slawinski, M.A., *Waves and rays in elastic continua*, World Scientific, 2013.

Slawinski, M.A., *Waves and rays in elastic continua*, 3rd ed., World Scientific, 2015.

Slawinski, M.A., *Waves and rays in seismology: Answers to unasked questions*, World Scientific, 2016.

Thomsen, L., Weak elastic anisotropy, *Geophys.*, **51**, 10, 1954–1966, 1986.

Voigt, W., *Lehrbuch der Kristallphysics, Teubner*, Leipzig, 1910.

Wilkinson, J.H., Eigenvalues of matrices of condensed forms. *The Algebraic Eigenvalue Problem*, (pp. 413-484). Oxford: Oxford University Press, 1965.